Award Number: W81XWH-18-2-0061

TITLE: **Intravenously Infusible Nanoparticles to Stop Bleeding and Increase Survival Following Trauma**

PRINCIPAL INVESTIGATOR: Erin Lavik

CONTRACTING ORGANIZATION: Maryland, University of, Baltimore County
BALTIMORE, MD 21250-0001

REPORT DATE: October 2020

TYPE OF REPORT: Annual

PREPARED FOR: U.S. Army Medical Research and Materiel Command
Fort Detrick, Maryland 21702-5012

REPORT DOCUMENTATION PAGE

Form Approved
OMB No. 0704-0188

1. REPORT DATE	2. REPORT TYPE	3. DATES COVERED
October 2020	Annual	9/30/2019-9/29/2020

4. TITLE AND SUBTITLE

Intravenously Infusible Nanoparticles to Stop Bleeding and Increase Survival Following Trauma

5a. CONTRACT NUMBER

5b. GRANT NUMBER
W81XWH-18-2-0061

5c. PROGRAM ELEMENT NUMBER

6. AUTHOR(S)

Erin Lavik

E-Mail: elavik@umbc.edu

5d. PROJECT NUMBER

5e. TASK NUMBER

5f. WORK UNIT NUMBER

7. PERFORMING ORGANIZATION NAME(S) AND ADDRESS(ES)

Maryland, University of, Baltimore County
1000 HILLTOP CIR
BALTIMORE MD 21250-0001

8. PERFORMING ORGANIZATION REPORT NUMBER

9. SPONSORING / MONITORING AGENCY NAME(S) AND ADDRESS(ES)

U.S. Army Medical Research and Materiel Command
Fort Detrick, Maryland 21702-5012

10. SPONSOR/MONITOR'S ACRONYM(S)

11. SPONSOR/MONITOR'S REPORT NUMBER(S)

12. DISTRIBUTION / AVAILABILITY STATEMENT

Approved for Public Release; Distribution Unlimited

13. SUPPLEMENTARY NOTES

14. ABSTRACT

Trauma induced bleeding is a major cause of fatality between ages 1 to 44, accounting for up to 50% of combat deaths. An immediate on-field intervention that can augment hemostasis can provide the scope of limiting uncontrollable bleeding and saving lives. While nanotherapeutics like hemostatic nanoparticles, that mimic the activity of fibrinogen, have shown promise in small animal models, translation to large animal models is often limited due to infusion reactions from systemic administration. We have worked on understanding and tuning the surface of the nanoparticles to overcome such a complement-mediated response. Over the last year, we have worked on a sensitive screening tool for complement activation due to nanoparticles and using that assay, we have pinned down the optimum stealth properties. The stealth hemostatic nanoparticles were deployed in an in vivo porcine trauma model to validate the safety and efficacy of the hemostatic nanoparticles.

15. SUBJECT TERMS

None Listed

16. SECURITY CLASSIFICATION OF:			17. LIMITATION OF ABSTRACT	18. NUMBER OF PAGES	19a. NAME OF RESPONSIBLE PERSON
a. REPORT	b. ABSTRACT	c. THIS PAGE			USAMRMC
U	U	U	UU	25	19b. TELEPHONE NUMBER *(include area code)*

Table of Contents

Page

Introduction

Trauma induced bleeding is a major cause of fatality between ages 1 to 44, accounting for up to 50% of combat deaths, and, in case of catastrophic trauma incidents, an immediate on-field response can provide the scope of controlling exsanguination and saving lives by prolonging the time to move and stabilize the patient. [1-4] Controlling hemorrhage is the first step in managing casualties, and while first responders can play a role in controlling external bleeding through pressure dressing and tourniquets, in case of internal bleeding, when intravenous hemostats such as recombinant factor rFVIIa, blood-derived components are required, the application is not possible until a medical facility is reached. To address such limitations, we have developed hemostatic nanoparticles to augment hemostasis mimicking the activity of fibrinogen. The hemostatic nanoparticles consist of a polyester core, with poly(ethylene glycol) corona, with a peptide sequence GRGDS conjugated to it. The peptide motif binds with glycoprotein IIb/IIIa in the activated platelets and helps in forming clots faster to reduce bleeding.[5-6] The nanoparticles can reduce bleeding by almost 50% and improved survival significantly in major femoral artery injury models for rodents following intravenous administration.[6] Moreover, the hemostatic nanoparticles are designed such that they are safe and stable at room temperature.[7] Administering the hemostatic nanoparticles after traumatic injury due to blasts can mitigate internal bleeding and improve the pathologic outcomes as well.[8] However, in large animals, it can trigger the complement system even at very low dosages.[9] This complement-mediated response, often termed as infusion reaction [10-11], is of concern for many other organic and inorganic nanoparticle systems as well.[9-10, 12-17]
The complement system, the first-in-line defense of the immune system against pathogens, is active at all times controlled by several complement regulators. However, uninhibited complement activation may eventually lead to inflammatory responses as severe as anaphylaxis, an acute life-threatening respiratory failure.[18] As the complement system attacks all components that are not recognized as healthy or familiar, nanomedicines such as the hemostatic nanoparticles may elicit complement-mediated initial infusion reactions as well. Such immune response leads to vasodilation, increased tissue permeability, edema, and drastic fall in blood pressure leading to shock, with symptoms appearing in minutes after exposure to an allergen and can occur within 30 minutes.[19-20]

Our previous work has shown that controlling zeta-potential leads to reduced complement activation at specific dosages for the hemostatic nanoparticles. As such, the objective of this work is to develop stealth hemostatic nanoparticles to overcome the complement-mediated hypersensitivity reactions and validate its efficacy in large animal trauma models. As the first step, we have focused on understanding the surface properties critical in overcoming the hypersensitivity response. We have studied the nanoparticles in vitro for their complement activity in human blood and determined the optimum stealth properties. Once the optimum stealth properties are determined, the nanoparticles were assessed in a large animal trauma model. The trauma model involved intravenous (IV) administration of hemostatic nanoparticles in a large animal (swine) pressure-targeted hemorrhagic shock polytrauma model. The reason behind choosing the porcine models for such studies is mainly the anatomic and histopathologic similarities with humans, and as porcine animals show activation for the same dosages as complement reactive humans, porcine animals are a feasible option for this study to validate the efficacy of the hemostatic nanoparticles without provoking hypersensitivity reactions. The outcomes of this study will play a critical role in designing clinically translatable hemostatic nanoparticles while maintaining its safety and efficacy.

Keywords

C5a, Complement, Coagulation, Hemostasis, PEGylation

Body

Key Research Accomplishments

Specific Aim 1: Determine the hemostatic efficacy and complement response to hemostatic nanoparticles in vitro as a function of hemostatic nanoparticle concentration

Specific Aim 2: Perform a pilot study to test the efficacy and safety using intravenous (IV) administration of hemostatic nanoparticles in a large animal (swine) pressure-targeted hemorrhagic shock polytrauma model

Specific Aim 3: Confirm the mechanism of augmented hemostasis

Task 1: Confirm that hemostatic nanoparticles do not activate complement over a range of doses

In the first task, our aim was to confirm that the hemostatic nanoparticles do not elicit any unwanted hypersensitivity reactions. Like many other nanomaterials, PLGA based hemostatic nanoparticles may lead to hypersensitivity reactions, especially in large animal models.[21] Previous work with the hemostatic nanoparticle has shown that highly negative or highly positive nanoparticles cause complement activation leading to vasodilation. [21] Further investigation revealed that tuning the zeta-potential of the nanoparticles can be a route to modulate such hypersensitivity responses.[21] As a result, our current efforts are directed towards designing stealth hemostatic nanoparticles that do not cause a complement-mediated hypersensitivity reaction. To do so, we first focused on determining the stealth design and validating the stealth property in vitro through complement assays using human blood matrices. The stealth design was determined through understanding the surface properties and its correlation with complement activation mediated hypersensitivity reactions. As zeta-potential, a surface property can impact complement activation we focused on further studying surface modifications and its impacts. One potential route of surface modification is introducing densely packed surface architecture to evade complement activation. Particles with brush-like polyethylene oxide (highly dense) or dense dextran brushes are more resistant to binding complement proteins compared to their counterparts with mushroom-like/ or lightly enveloped surfaces.[22-23]

The hemostatic nanoparticles have a polyester core with poly(ethylene glycol) (PEG) corona to which, the peptide motif GRGDS is bioconjugated. We have worked on varying ratios of PEG on the surface of the hemostatic nanoparticles to investigate the impact of surface architecture. The objective was to fabricate hemostatic nanoparticles with surface containing different ratios of PEG as well as blending different lengths of PEG linkers. Hence, poly(lactic acid) based hemostatic nanoparticles were prepared by blending synthesized poly(l-lactic acid)-*b*-poly(ethylene glycol) (PLLA-PEG) block copolymer poly(d-lactic acid)-*b*-poly(ethylene glycol) (PDLA-PEG). As described before, first, PLLA-PEG, PDLA-PEG, and PDLA were synthesized through ring-opening polymerization. [7, 24] To prepare the nanoparticles, the polymer dissolved in the organic phase at a concentration of 20mg/ml was added dropwise to double the volumetric amount of phosphate-buffered saline and stir hardened. The particles were characterized through dynamic light scattering for determining the hydrodynamic diameter and the zeta-potential.

As the first step, we synthesized nanoparticles with different amounts of PEG on the surface to understand how it impacts changes in complement protein C5a in vitro. Table 1 summarizes the observed zeta-potential in dilute potassium chloride solution and the hydrodynamic diameter of the nanoparticles suspended in PBS.

Table 1: Summary of nanoparticles used for the ELISA assays

Type	Formulation	Size (nm)	Zeta Potential (mV)
10%PLLA-PEG	90%PDLA+10%PLLA-PEG	284.3±2.122	-20.9±1.1
50%PLLA-PEG	50%PDLA+50%PLLA-PEG	517.9±8.958	-18±1.18
75%PLLA-PEG	25%PDLA+75%PLLA-PEG	383.2±11.92	-15.2±1.33
100%PLA-PEG	75%PLLA-PEG+25%PDLA-PEG	387.2±2.9161	-15.6±1.12

The biomarker chosen for tracking the complement activation in vitro was the fragment C5a generated due to the depletion of C3. Complement activation leads to initial C3-convertase formation, and the convertase catalyzes the breakdown of C3 into the smaller fragment C3a and larger fragment C3b.[25-27] The pathway proceeds generating anaphylatoxins and the eventual terminal complex that works on clearing the threat out of the system.[25-27]The anaphylatoxin C5a is a potent inflammatory molecule that targets immune and non-immune cell receptors and leads to vasodilation, increased cell permeability, and contraction of smooth muscles.[27]

Once the nanoparticles were fabricated, these were incubated with heparinized human whole blood. The nanoparticles were added at a dosage of 0.25mg/ml. As positive control, zymosan a known complement activator, was used at same dosage. The nanoparticle suspension in Dulbecco's PBS(PBS) (without Ca and Mg) at required dosage was gently pipetted with blood and incubated at 37 °C for 45 minutes. The plasma was separated immediately by centrifuging at 4000g for 5 minutes and stored on ice until the assays were run. The samples were diluted as required following the assay protocols. The fold change compared to amount of C5a in whole blood incubated with PBS without any nanoparticles or zymosan was determined. The normalized changes for the nanoparticles are shown in figure 1.

The normalized change was determined compared to the amount of C5a in samples incubated with phosphate-buffered saline. C5a generation was lower for nanoparticles with the greatest density of PEG on the surface, while lower amounts of PEG on the surface had led to a higher change in C5a. Therefore, while moving to the next stage of the project, the formulation selected based on the least amount of C5a generation was the nanoparticles with the highest amount of PEG, which is the batch of nanoparticle prepared by blending 75%PLLA-PEG (with 5000 Da length PEG) and 25% PDLA-PEG (with 3400 Da PEG). The difference in length is later utilized to extend out the peptide motifs using the 5000Da PEG from the surface of the nanoparticles.

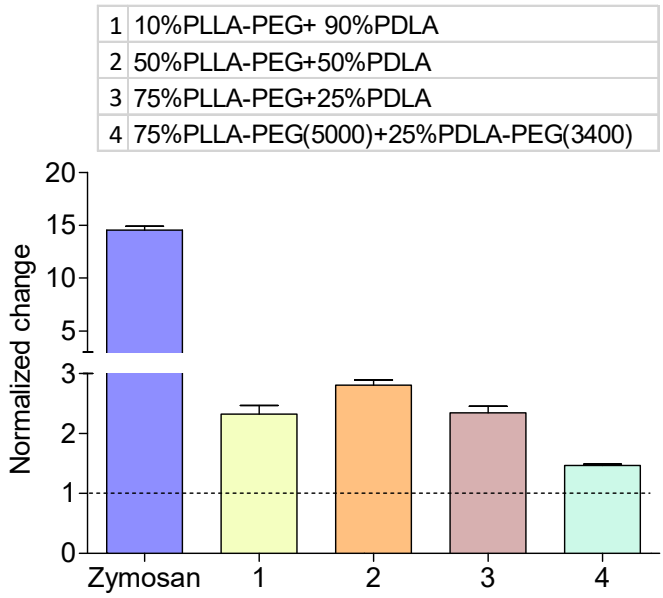

Figure 1: Normalized change in C5a in human whole blood with changing ratios of PLLA-PEG to PDLA or PDLA-PEG. The dashed line represents baseline for the negative control PBS and value in parentheses indicate the molecular weights of the PEG unit.

The impact of PEGylation was further assessed and confirmed in the hemostatic nanoparticles synthesized with peptides conjugated to it. Two peptide motifs cRGDyK and GRGDS were investigated and as blood matrix for generating the response, complement-protected human serum was used. For conjugating the peptide motif responsible for the hemostatic activity, the peptide motif of interest was bioconjugated to PLLA-PEG through NHS/EDC zero-length linker.[7] The in vitro assay for quantifying the complement changes was carried out as mentioned above. The normalized change in comparison to serum incubated with PBS is shown in figure 2. The normalized change was the least for nanoparticles containing the cRGDyK peptide motif. However, the difference in fold change between nanoparticles with GRGDS and nanoparticle with cRGDyK was very small. The peptide conjugated nanoparticles had lesser C5a fold change than control nanoparticles, which could be due to the zeta-potential getting further lowered.

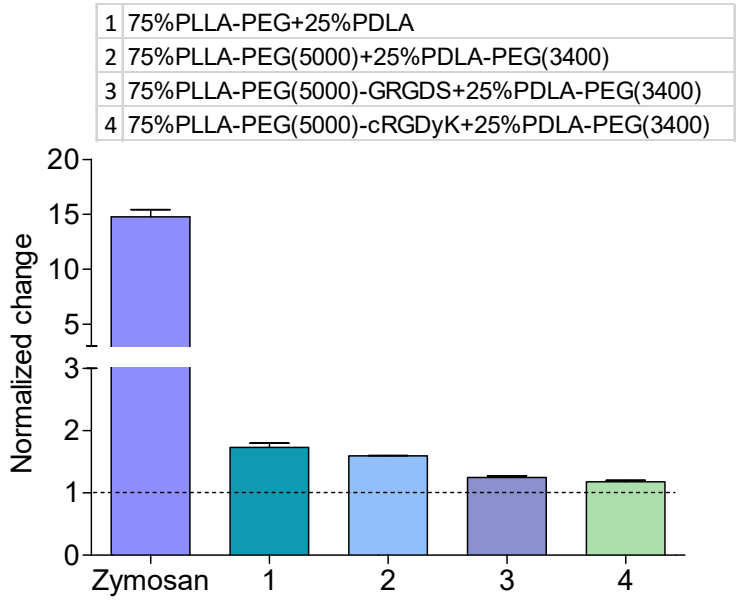

Figure 2: Normalized change in C5a for the peptide conjugated nanoparticles with increased amount of PEG on surface. The dashed line represents baseline for the negative control PBS and value in parentheses indicate the molecular weights of the PEG unit.

Thus, in the first task, we determined that a higher amount of PEGylation was able to reduce the change in complement protein C5a in vitro in whole blood and serum. Hence based on the results, for the in vivo large animal (swine) pressure-targeted hemorrhagic shock polytrauma model, as stealth nanoparticles, the PLA-PEG nanoparticles with the highest amount of PEG on the surface were chosen. Treatment batches were prepared using the GRGDS peptide motif, while control batches were devoid of the peptide motif. The average size of the batches used for the in vivo study is summarized in the table below:

Table 2: Summary of hydrodynamic diameter and zeta-potential of the hemostatic PLA-PEG nanoparticles with peptide motif GRGDS and control PLA-PEG nanoparticles

Type of Nanoparticle	Z-Average (nm)	Zeta-potential (mV)
Hemostatic nanoparticles	367.5±28.8	-13.7±1.0
Control nanoparticles	334.1±18.9	-15.5±0.4

Task 2: Perform a pilot study to test the efficacy and safety using intravenous (IV) administration of hemostatic nanoparticles in a large animal (swine) pressure-targeted hemorrhagic shock polytrauma model

The study protocol for the IV administration of the hemostatic nanoparticles in the large animal (swine) pressure-targeted hemorrhagic shock polytrauma model was prepared by the Naval Medical Research Unit, and the proposed study was approved by the 711th HPW/RHD JBSA-Fort Sam Houston Institutional Animal Care and Use Committee (IACUC) in compliance with all applicable Federal regulations governing the protection of animals in research. All procedures were performed in facilities accredited by the AAALAC international. A standardized grade III liver injury model based on Gurney et al. was used. The injury model would result in ~25% lobectomy, and 5 minutes post-injury, the treatment or control infusion will be administered. The objective of this study was to investigate whether the nanoparticles with stealth properties in vitro cause any adverse reaction in vivo. The animal study consisted of two arms: Injured and uninjured arm. The injured arm had three subgroups: Vehicle control arm receiving 0.9% NaCl normal saline (n=6), control arm receiving control nanoparticles at a dosage of 2mg/kg (n=6), and treatment arm receiving the hemostatic nanoparticles at a dosage of 2mg/kg (n=7). The uninjured arm had three subgroups: Vehicle control arm

receiving 0.9% NaCl normal saline (n=3), control arm receiving control nanoparticles at a dosage of 2mg/kg (n=3), and treatment arm receiving the hemostatic nanoparticles at a dosage of 2mg/kg (n=3).

The timeline of the study begins with baseline measurements of vitals as well as blood sample collection. With anticoagulant citrate phosphate dextrose adenine, 30% of total blood was also collected before the injury was made for infusion post-injury. Catheters were placed for administration of resuscitation fluids and treatment infusions, and pressure monitoring. Once injury was made, after 5 minutes of spontaneous bleeding, 30 mL bolus of either 1) 0.9% NaCl, 2) 2 mg/kg control nanoparticles, or 3) 2 mg/kg hemostatic nanoparticles were administered. At the end of the treatment phase, after 60 minutes of administration of the infusion fluids, the swine were under observation for 120 minutes. At the end of the timeline, swine were humanely euthanized at T=180 min with pentobarbital sodium and phenytoin sodium (Euthasol®, 390 mg/mL, Virbac Corporation, Fort Worth, TX, USA) During the study; whole blood was drawn for arterial blood gas, complete blood count, serum chemistries, rotational thromboelastometry (ROTEM), and STAGO at BSLN, TRAU, T=0min, 15min, 30min, 45min, 60min, 120min, 180min (fig 3).

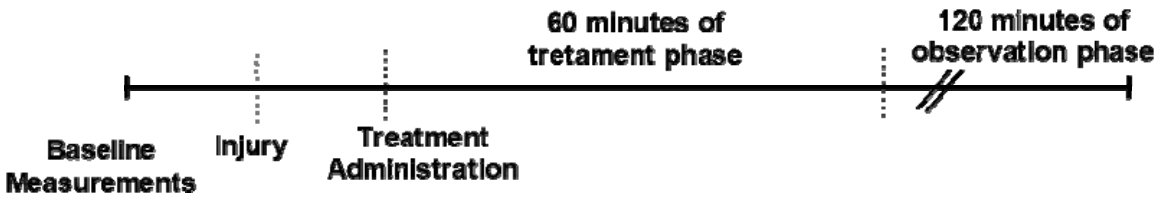

Figure 3: Timeline of the study conducted for IV infusion of hemostatic nanoparticles in the large animal (swine) pressure-targeted hemorrhagic shock polytrauma model.

Survival in the injured and uninjured arm

The survival rate in the uninjured and uninjured arms are summarized in the table below:

Table 3: Survival rate in the injured and uninjured arms of the study

Arm	Subgroup	Survival rate (%)
Injured Arm	Vehicle Control (n=6)	100
	Control Nanoparticles (n=6)	66.7
	Hemostatic Nanoparticles (n=7)	57.1
Uninjured Arm	Vehicle Control (n=3)	100
	Control Nanoparticles (n=3)	66.7
	Hemostatic Nanoparticles (n=3)	100

Analyzing the complete blood count results for injured and uninjured cohorts

White Blood Cells

At the time of trauma, the white blood cell levels were lower than the baseline measurements (Figure 4). The values increased over the 5 minutes of hemorrhaging in the vehicle control groups (n=5/6), control nanoparticles groups (n=4/6) and the hemostatic nanoparticle groups (n=4/6). The highest change (2.5 times of baseline measurement) in WBCs was observed in one of the animals in the HNP group at the end of the treatment phase, while the rest of the animals in the groups showed a similar trend. In the uninjured cohort, all the animals in the vehicle control, hemostatic nanoparticle group as well as the control nanoparticle group showed higher normalized changes in the white blood cell levels. The initial drop in the injured cohort between baseline measurement and trauma could be due to the collection of 30% of the femoral blood for using as resuscitation fluid later.

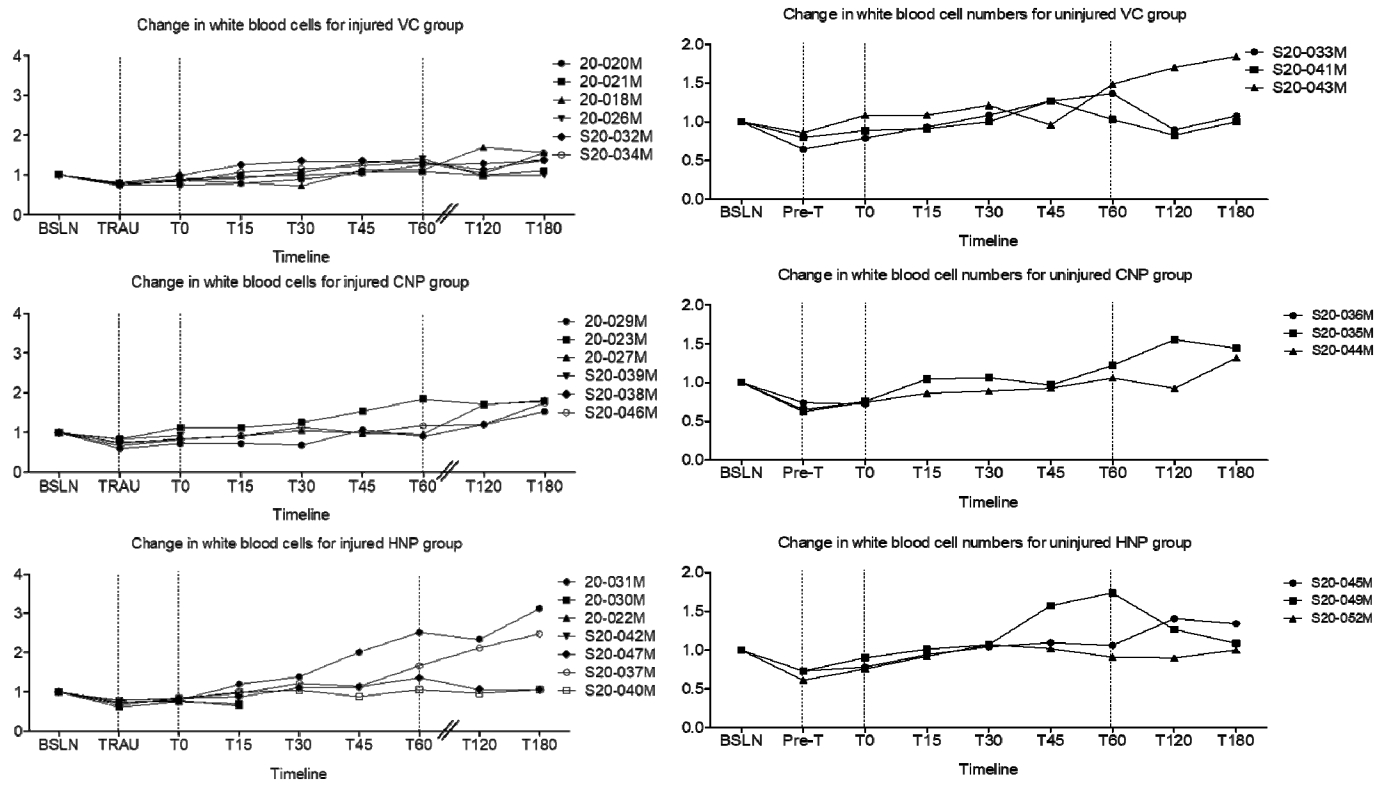

Figure 4: Change in white blood cells in the injured and uninjured cohort

Platelets

In the injured cohort, the change is similar for vehicle control and the control nanoparticles between the timepoints T0 (time of injecting nanoparticles) and T15 (15 minutes after injection). The platelet drops for hemostatic nanoparticle group (n=3/6) within the mentioned time. For the uninjured cohort, the trend in change is not significantly different between the three groups between T0 and T15 (Figure 5).

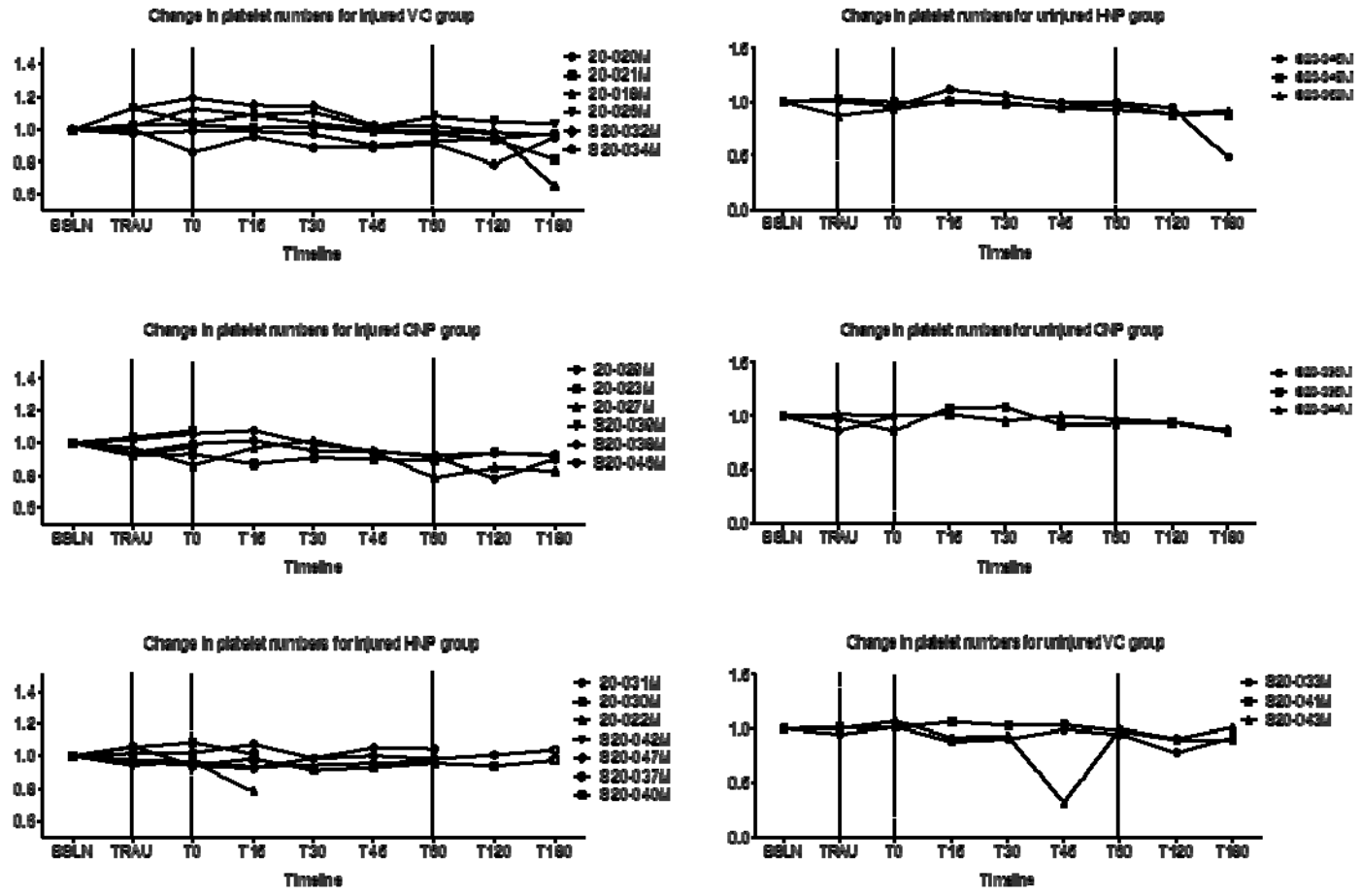

Figure 5: Change in platelet level for injured and uninjured cohort

Lymphocytes

Between T0 and T15, lymphocyte levels did not change significantly between the three groups in the injured cohort. The lymphocytes surged at the end of the treatment for 2 animals in the hemostatic nanoparticle (HNP) group. The animals 20-031M and S20-037M also exhibited a surge in WBCs at the same timepoint. In the uninjured cohort, the trend range in the change of lymphocyte levels is similar among the three groups (Figure 6).

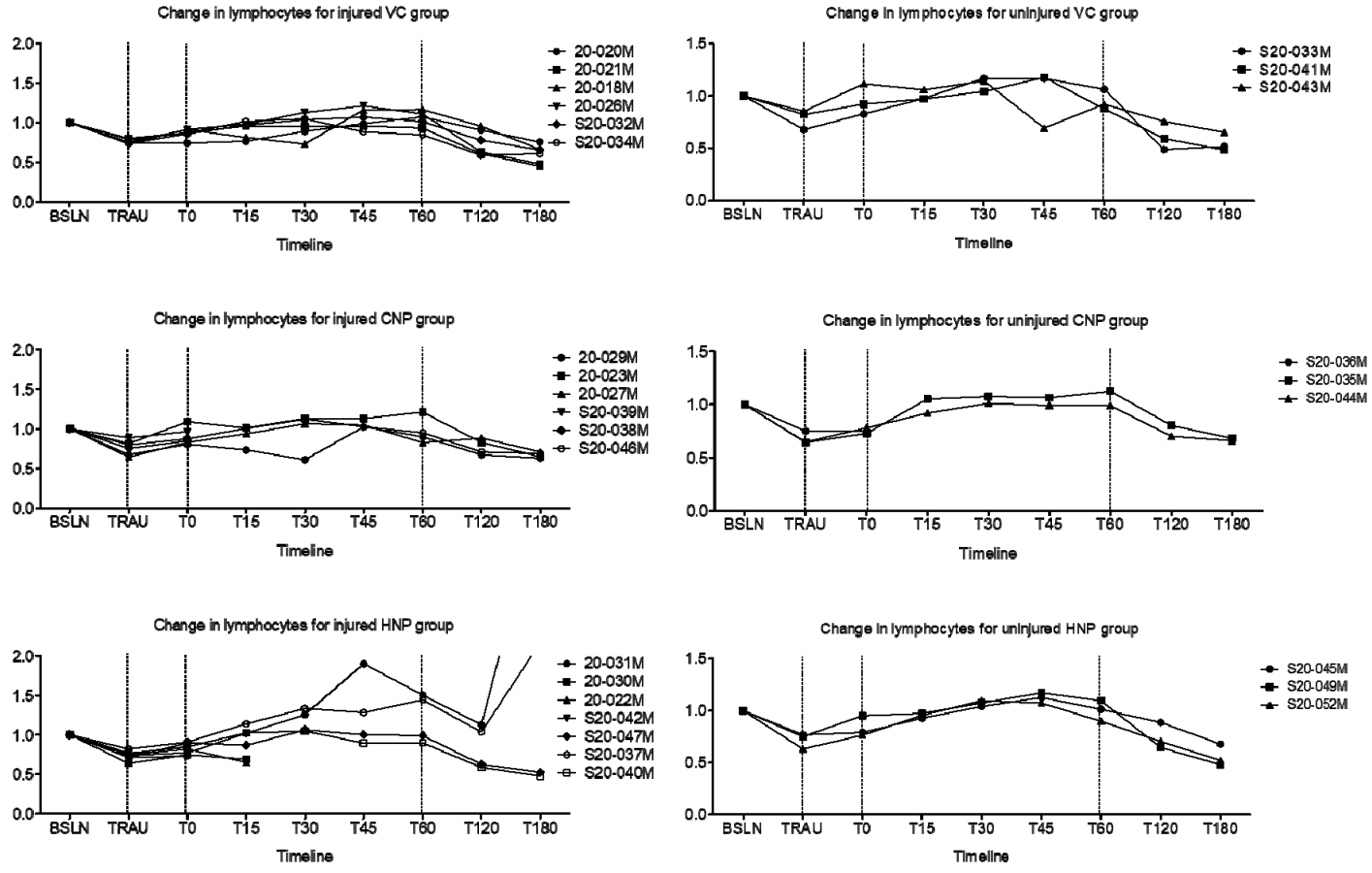

Figure 6: Change in lymphocyte levels in injured and uninjured cohort

Monocytes

One of the animals in the injured hemostatic nanoparticle (HNP) group (S20-037) exhibited drastic changes in monocytes, with the levels further elevating in the end of the treatment phase and during the observation phase. In the uninjured cohort, the groups receiving hemostatic and control nanoparticles showed fluctuations compared to vehicle control groups. However, the levels remained close to the baseline and were lower compared to the injured groups (Figure 7).

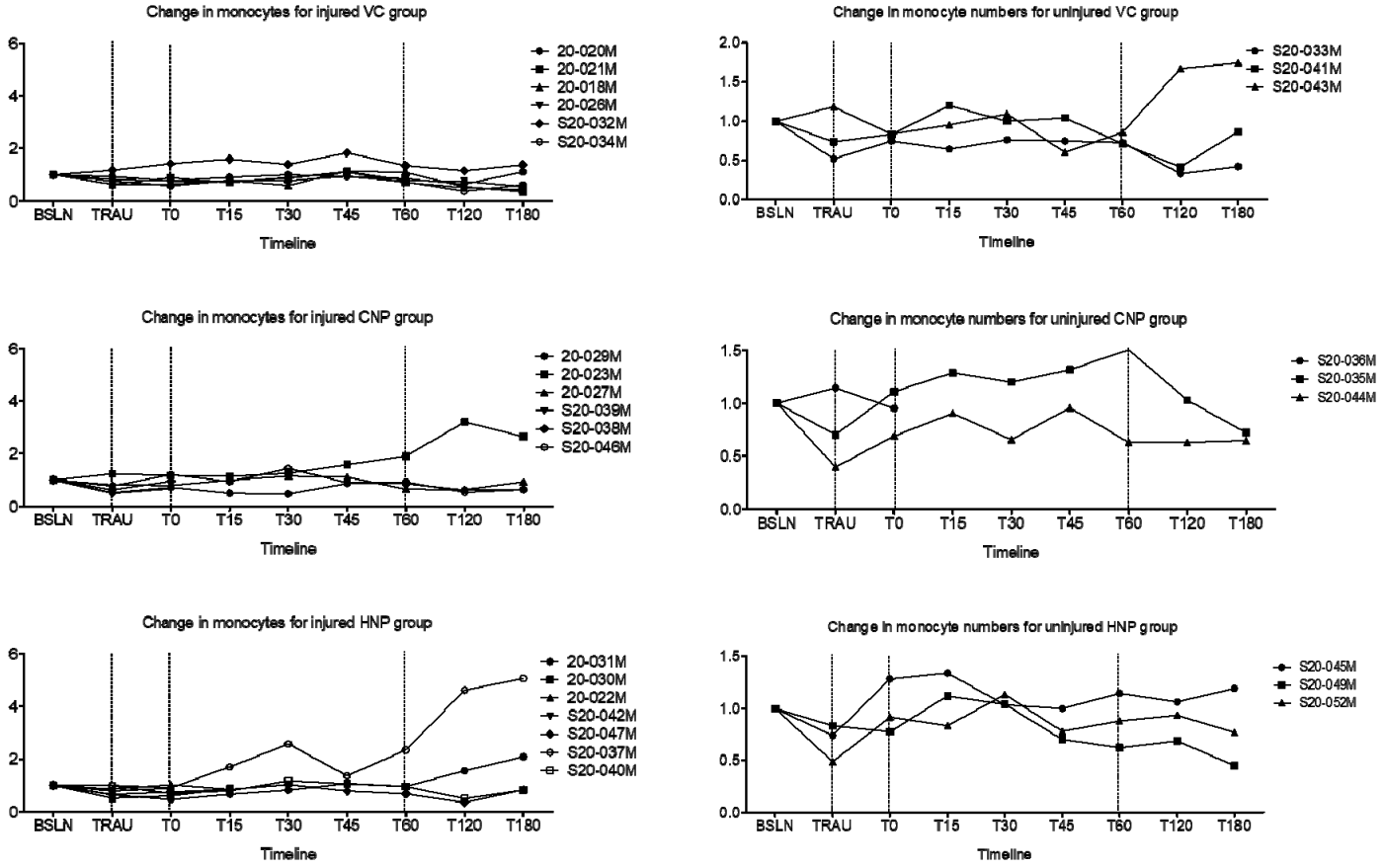

Figure 7: Change in monocytes in the injured and uninjured cohort

Neutrophils

The change in neutrophils was higher in the vehicle control group and the control nanoparticles (CNP) group in the injured cohort during the observation phase. At the initial time points between T0 and T15, the levels increased in the vehicle control group (n=5/6), control nanoparticle group (n=4/6) and hemostatic nanoparticle (HNP) group (n=3/7). In the uninjured cohort, changes were similar between the groups for the time between T0 and T15. One of the animals in the uninjured hemostatic nanoparticle (HNP) group showed the highest change (S20-045) (Figure 8).

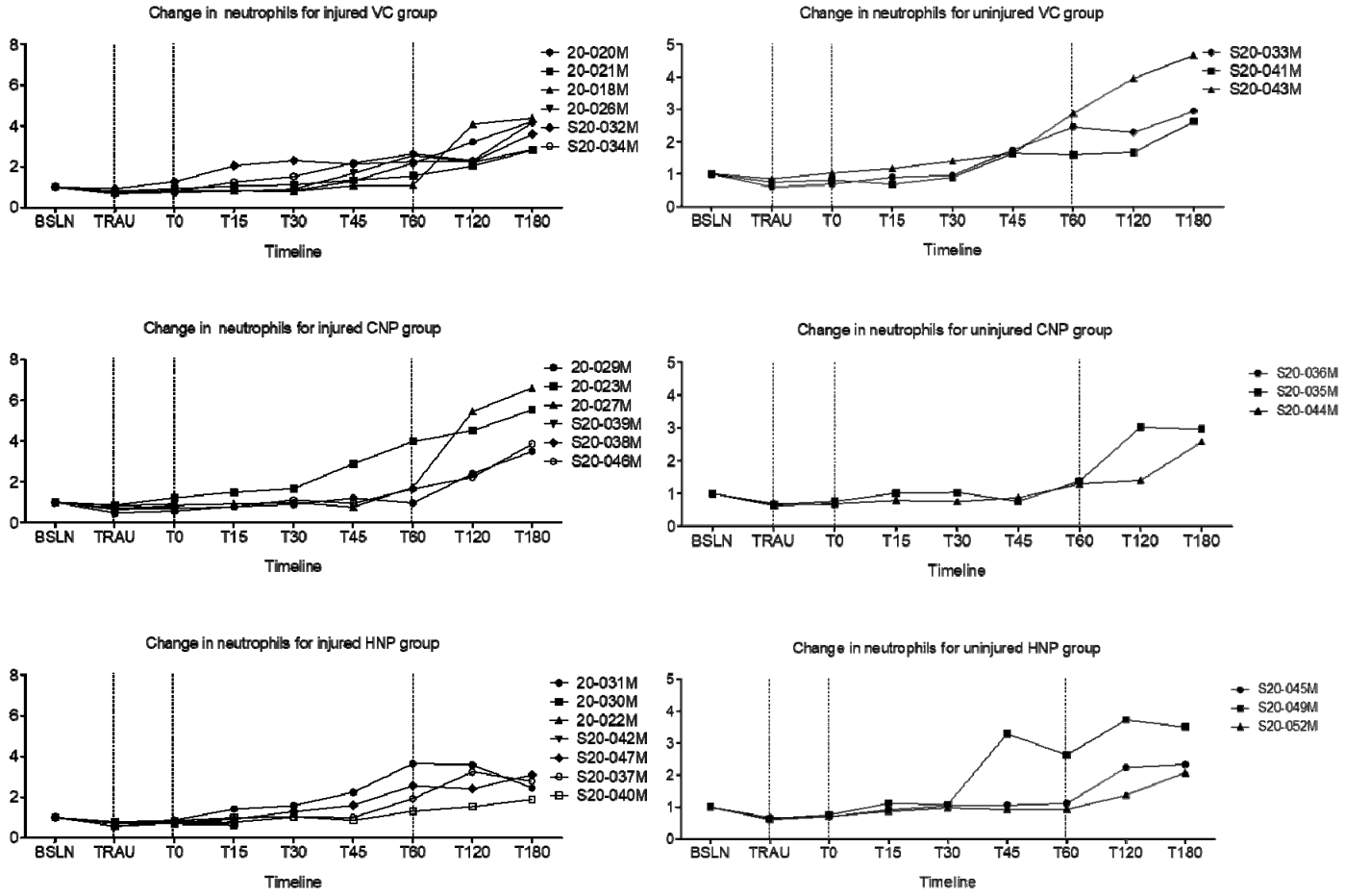

Figure 8: Change in neutrophil levels in the injured cohorts and uninjured cohorts

Eosinophils

Within the injured groups, the levels did not change significantly between T0 and T15. One of the animals in the injured hemostatic nanoparticle group (HNP) group that displayed elevated levels of lymphocytes and WBC, also exhibited a sudden increase after 30 minutes of infusion. In the uninjured group, the change was highest at the end of the treatment phase for one of the animals in the hemostatic nanoparticle group (S20-049) (Figure 9).

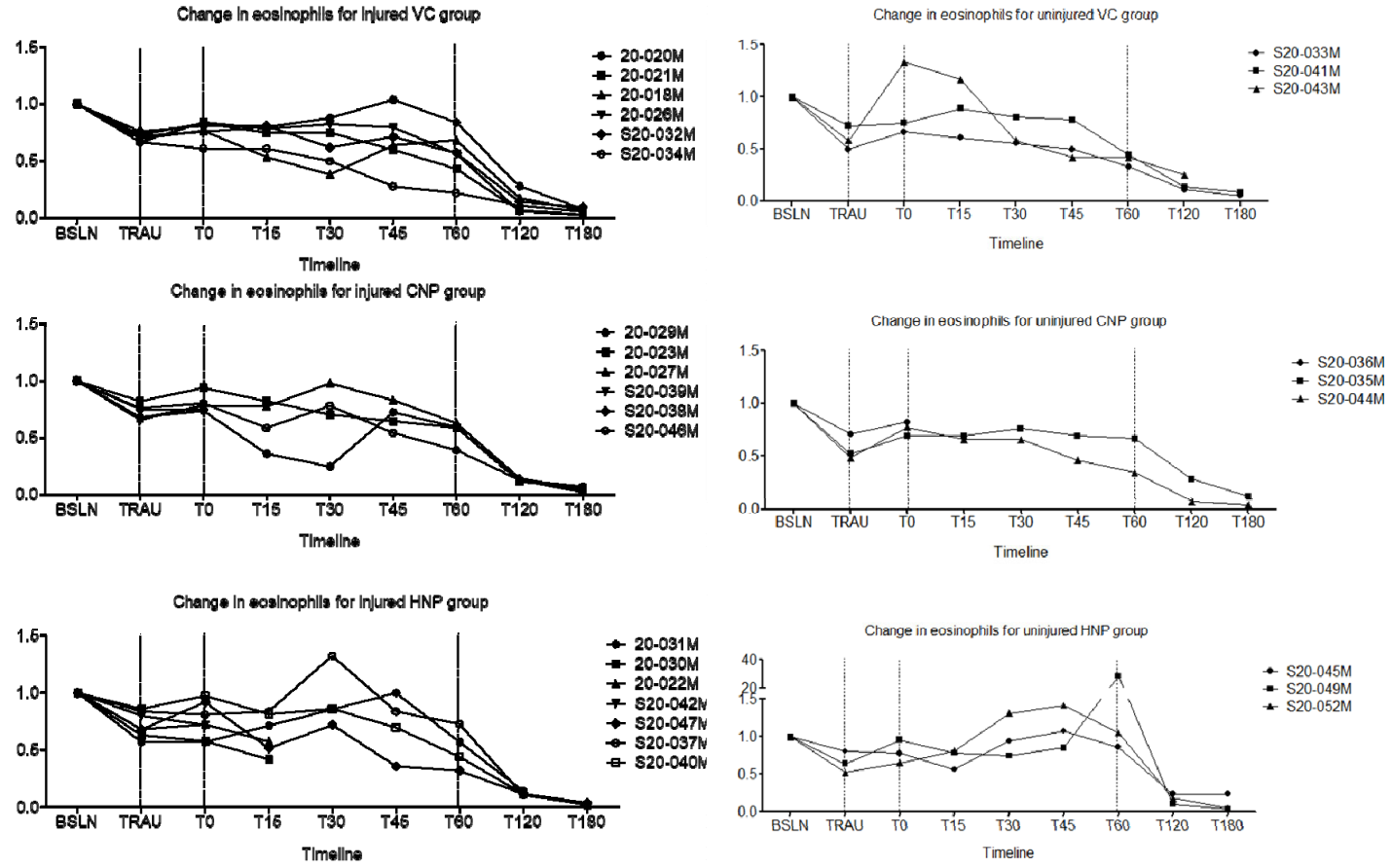

Figure 9: Change in eosinophils in the injured and uninjured cohort

Analyzing change in vitals over time for the injured and uninjured cohorts

The key monitoring parameter for signs of hypersensitivity reactions involve the cardiopulmonary vitals such as the heart rate, end-tidal CO_2 (ET CO_2), and the oxygen saturation (SpO_2), as these vitals are to change drastically showing signs of distress upon hypersensitivity reactions. Figures 10, 11, and 12 summarize the changes in the heart rate, ET CO_2, and the SpO_2 over the duration of the study. It is noted that compared to the vehicle control, the hemostatic and control nanoparticle groups in the injured cohort show similar pattern in the heart rate. The heart rate fluctuation is seen initially starting from the time of trauma in all the cohorts. The rise in the heart rate in case of the uninjured cohort, where the trauma is absent indicates that a part of this initial change in heart rate could be due to the 30% of blood drawn initially for using later as resuscitation fluid in the treatment phase in both the cohorts. The ET CO_2 and the SpO_2 levels remain close to 100% compared to baseline other than slight fluctuation in ET CO_2 that stabilizes within minutes.

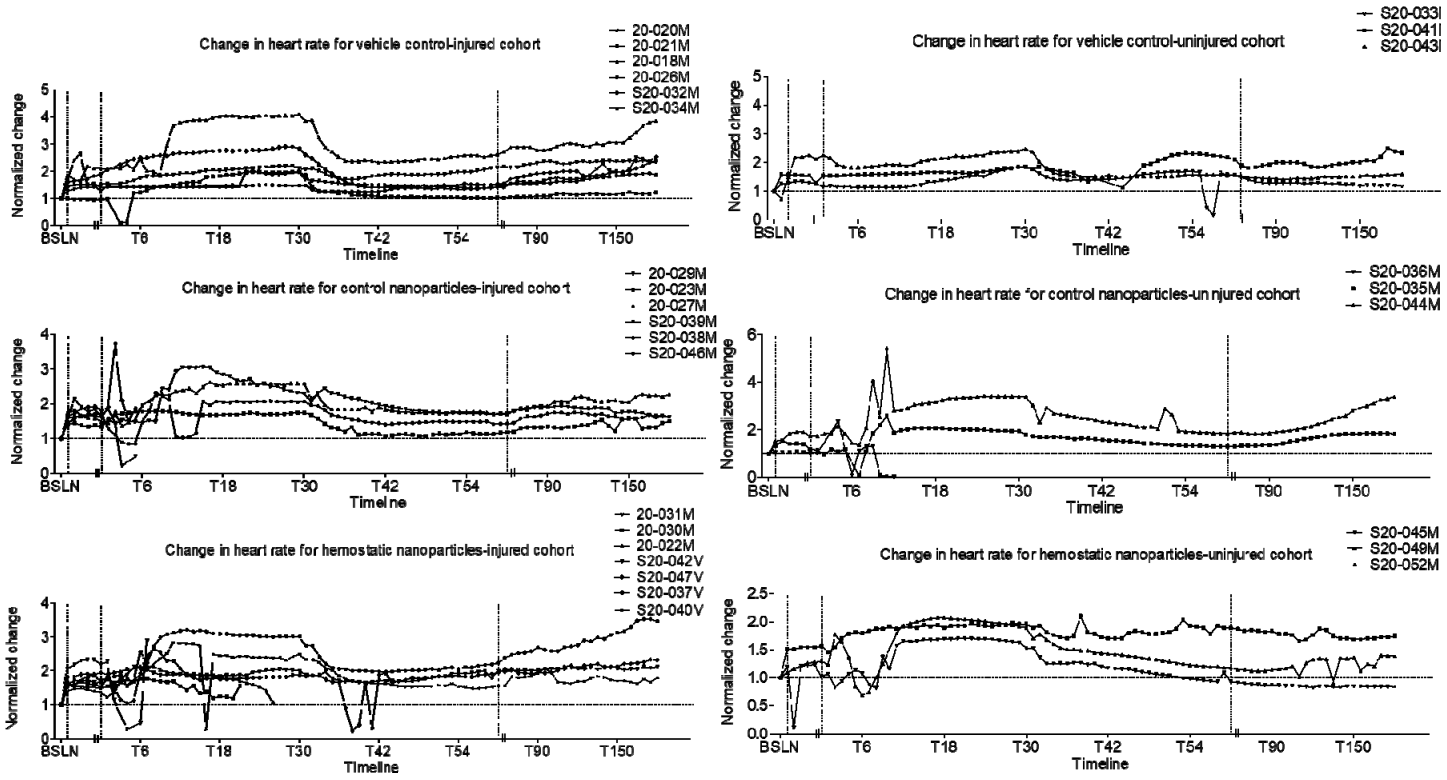

Figure 10: Normalized change in heart rate for the injured and uninjured cohort

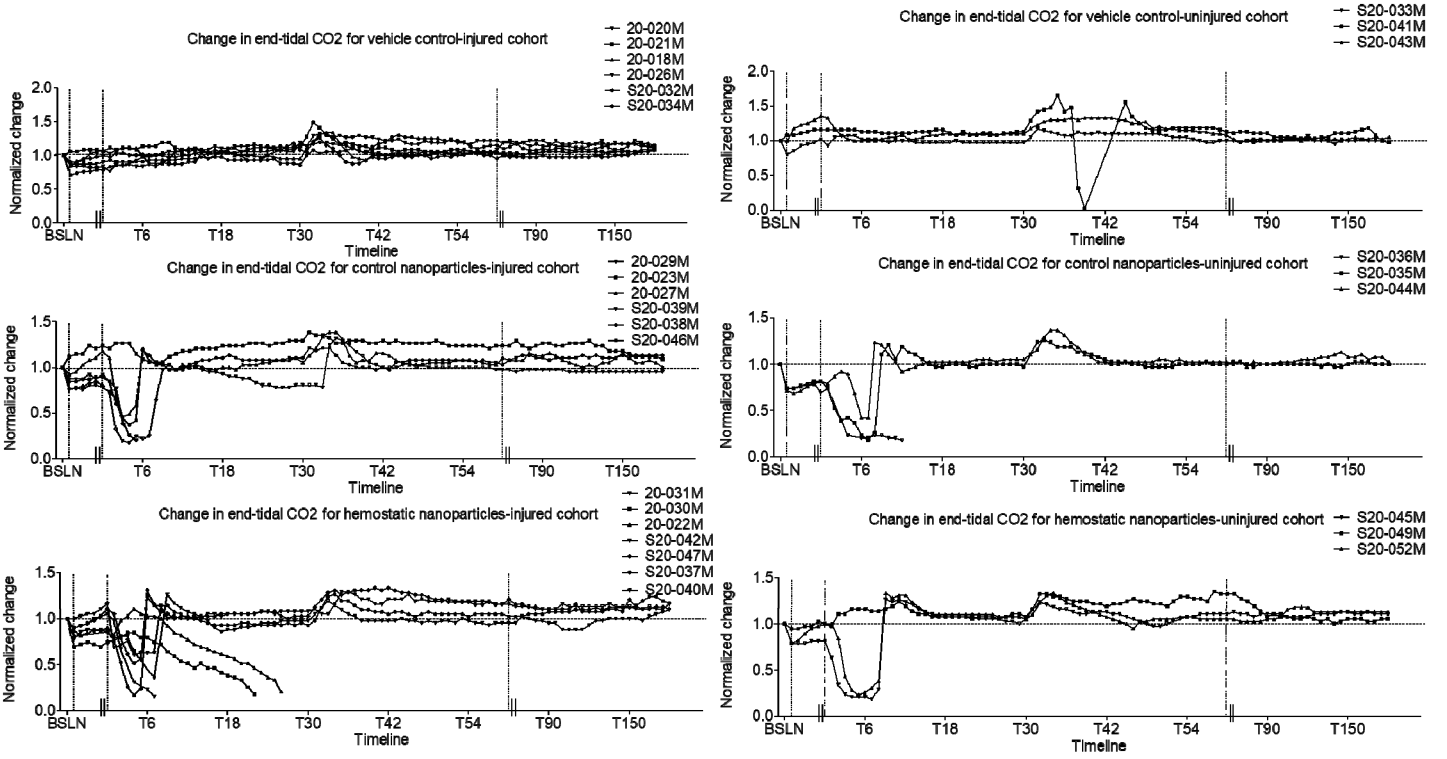

Figure 11: Normalized change in end-tidal CO2 for the injured and uninjured cohorts

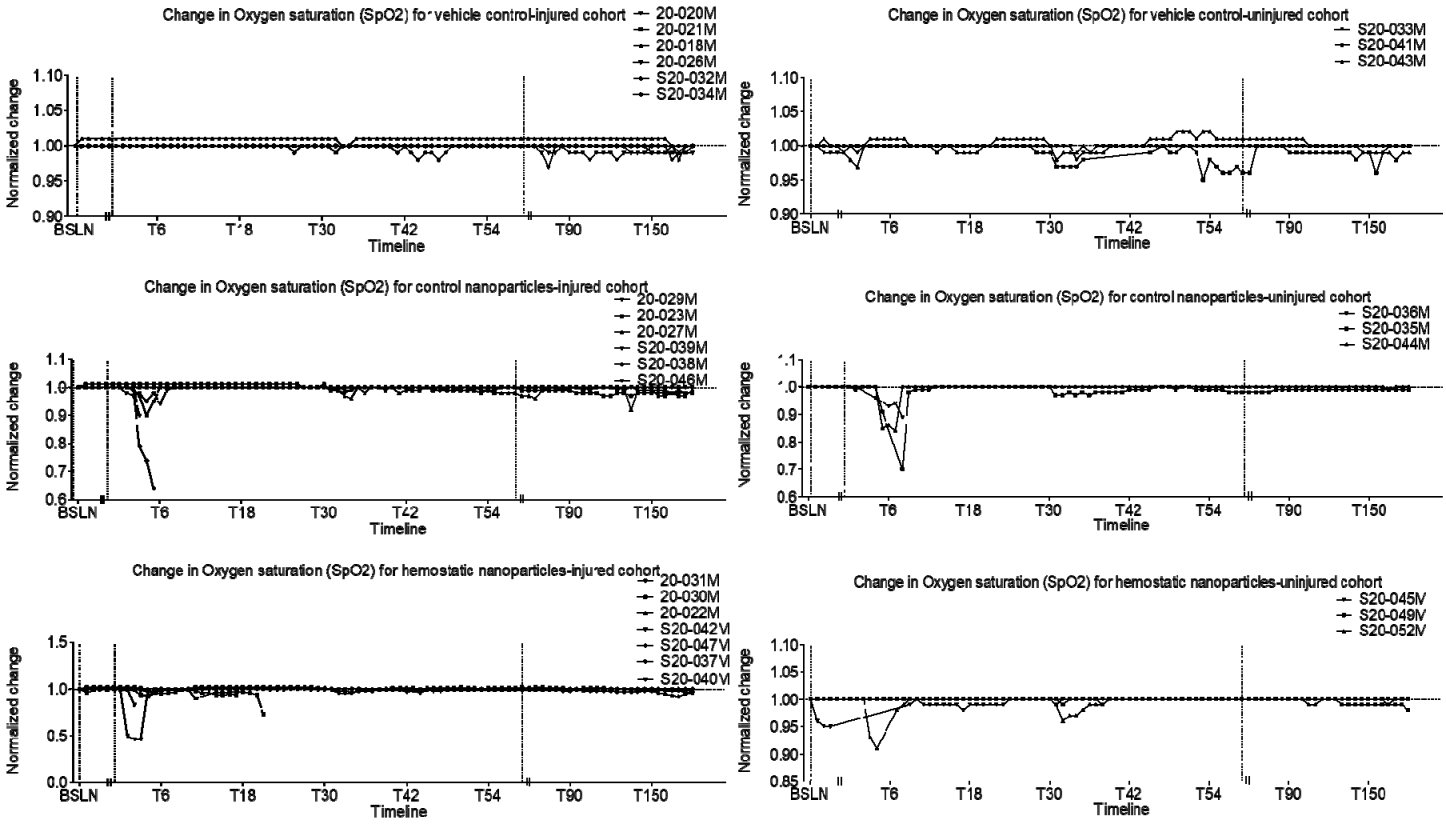

Figure 12: Change in SpO2 for the injured and uninjured cohorts

Analysis of ROTEM data from the porcine multi-trauma injury study to understand the efficacy of the hemostatic nanoparticles

For analyzing the ROTEM data, the summation of clotting time (CT) and clot formation time (CFT) was determined from the available data. The clotting time is the time required to reach initial clotting of 2mm, while CFT is the time between the formation of the 2mm clot and a clot of 20mm thickness. Hence, CT+CFT is the total time required for forming a 20mm clot. Previously, the parameter CT+CFT was evaluated for the PLGA-PLL-PEG-GRGDS hemostatic nanoparticles in vitro using citrated rat blood, and the CT+CFT decreased, with MCF increasing compared to saline.[6] The nonactivated NATEM test was used in that analysis.[6]

The ROTEM tests used for collecting data in the porcine trauma model were: EXTEM, FibTEM, and ApTEM. The test EXTEM uses tissue factor to initiate the extrinsic clotting cascade.[28] FibTEM is useful in monitoring the presence of fibrinogen, as the test uses cytochalasin D that inhibits platelet activity.[28] ApTEM on the other hand is an EXTEM assay that uses aprotinin to stabilize the clot against hyperfibrinolysis.[28] The hemostatic nanoparticles consist of a polyester core, with poly(ethylene glycol) corona, with a peptide sequence GRGDS conjugated to the PEG corona. The peptide motif binds with glycoprotein IIb/IIIa in the activated platelets and helps in forming clots faster to reduce bleeding mimicking activity of fibrinogen.[5-6] Thus, due to the particles mimicking the activity of fibrinogen, we looked into the changes in CT+CFT and the MCF for the injured and uninjured groups using the FibTEM data. The normalized changes for the parameters (CT+CFT) and MCF were determined compared to the values observed at baseline for each animal. The observations for CT+CFT are summarized below for the FibTEM test of ROTEM is summarized below in figure 1. It is observed that in the blood collected at time points from the injured animals, the normalized change in CT+CFT determined using FibTEM decreased over time from the time of infusion, for the observations at 45 minutes post infusion and onwards compared to control nanoparticles and vehicle control (i.e. normal saline) (Figure 13). The normalized change was close to the baseline and it decreased past 45 minutes for the hemostatic nanoparticles indicating that the particles are playing a role in supplementing the fibrinogen depletion following a trauma. In case of the uninjured groups, such a trend is not observed.

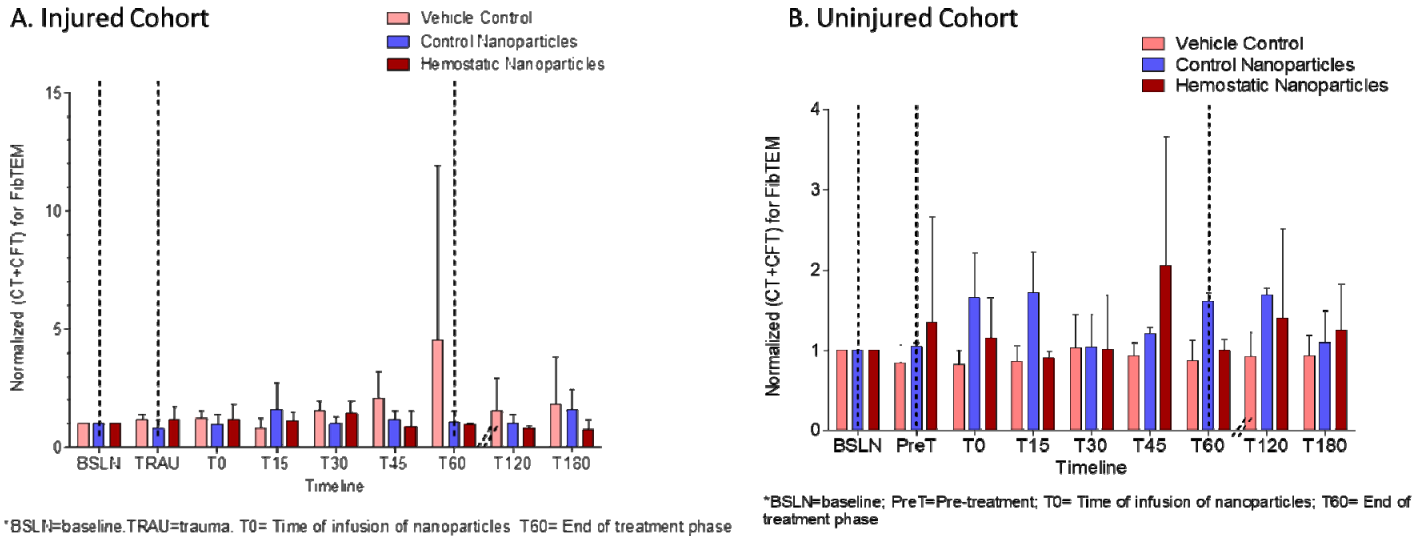

Figure 13: Normalized change in CT+CFT for the injured and uninjured cohorts

With the impact of trauma being heterogeneous for different animals, we also studied the trends in individual animals. The normalized change was calculated as before, compared to the baseline measurements recorded. The findings are summarized in Figures 2 and 3. In the injured vehicle control group, four out of six animals showed an increase in CT+CFT post-infusion. Whereas four animals survived the entire treatment phase in the injured control nanoparticles group, with CT+CFT increasing overtime for 3 out of those 4 animals. For the four out of seven animals that survived the entire treatment phase in the injured hemostatic nanoparticle group, CT+CFT decreased compared to baseline (Figure 14).

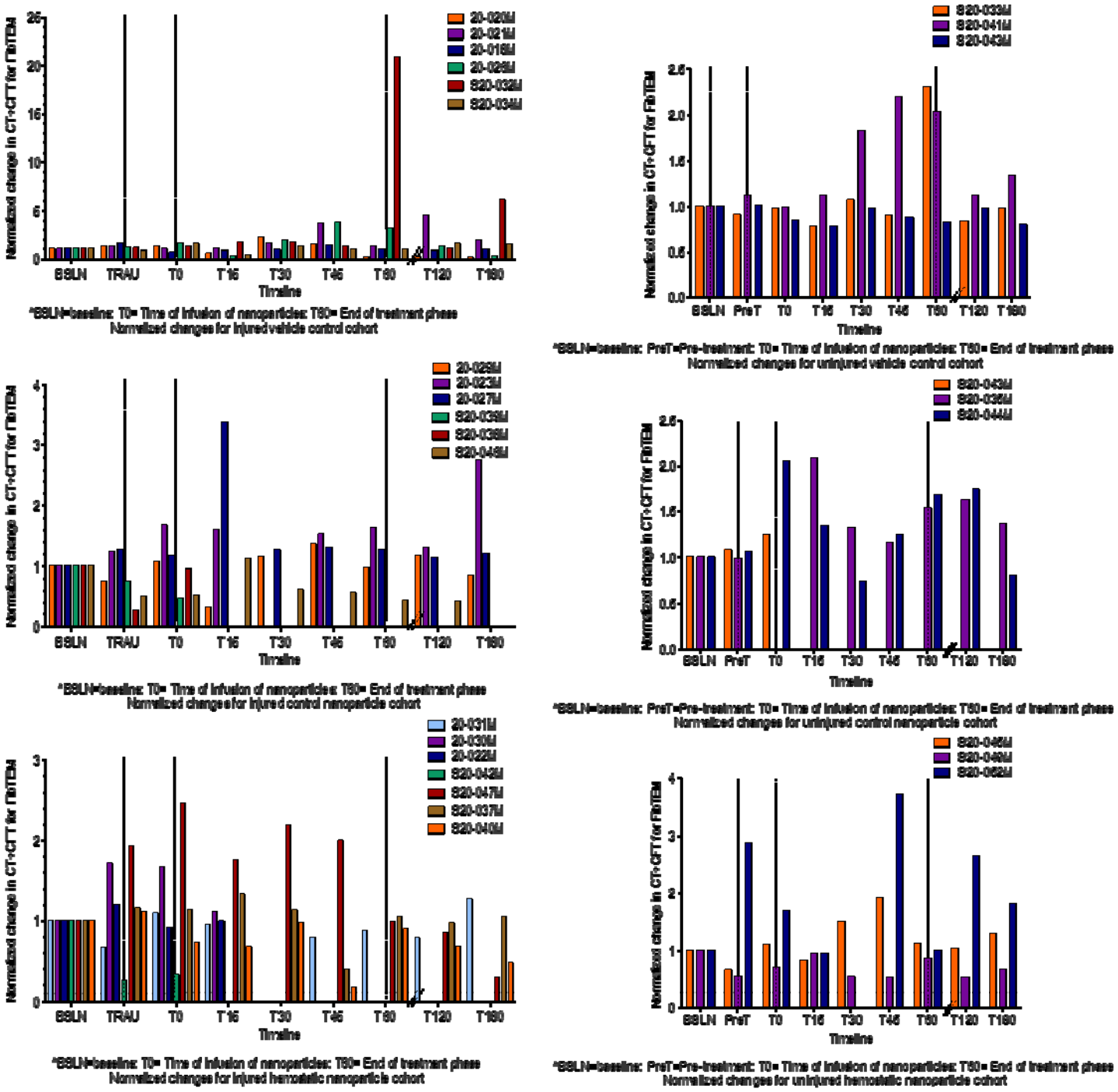

Figure 14: Normalized change in CT+CFT for each animal in the injured and uninjured groups

The maximum clot firmness in the vehicle control group changed drastically upon the infusion of saline when measured using FIBTEM, compared to baseline. (Figure 15). Out of the 4 animals that survived the treatment phase in the hemostatic nanoparticles group, 3 showed a slight increase in maximum clot firmness compared to the time of infusion T0.

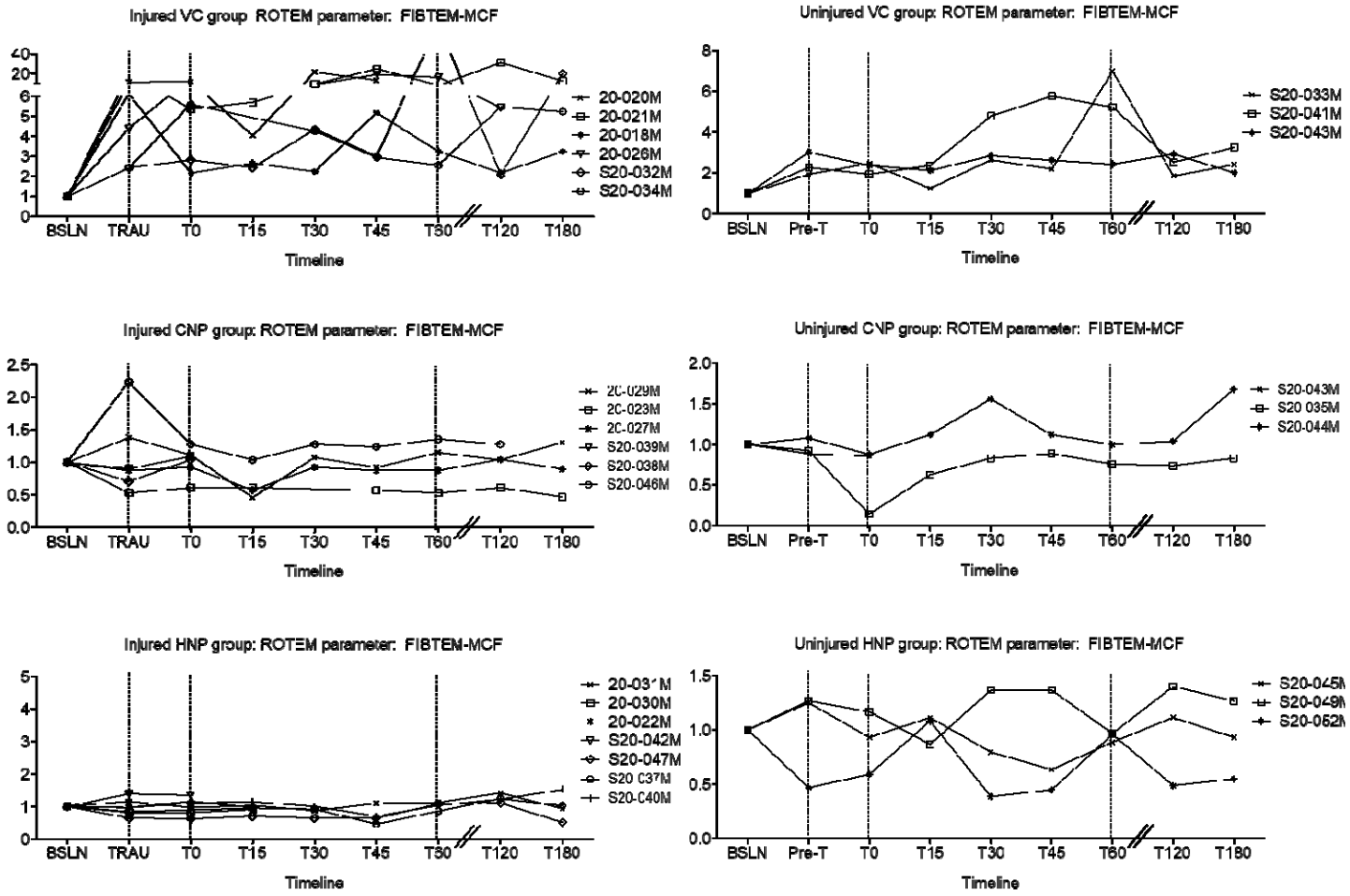

Figure 15: Normalized change in maximum clot firmness for injured cohort using FIBTEM

Analyzing the blood loss per body mass for the injured groups to understand the efficacy of the hemostatic nanoparticles

The blood loss for each animal was expressed in terms of ml/kg by dividing total blood loss by the animals' body weight. The results are summarized in figure 16. In the vehicle control group, the blood loss per unit body mass at the end of the treatment phase were 3.13, 4.67, 6.16, 7.18, 7.47 and 7.51 ml/kg with survival being 100%. For the control nanoparticles group, 4 out of 6 animals survived the treatment phase, with the blood loss being 2.25, 413, 5.39 and 5.99 ml/kg at the end of the treatment phase. However, 2 animals in the group exsanguinating exhibited high blood loss of 7.55 and 13.27 ml/kg, with blood loss increasing by 3-4.5-times 5 minutes after infusion. For the animals in the hemostatic nanoparticle group, 4 out of 7 animals survived. The animals had blood loss of 1.96, 2.62, 6.71 and 12.1 ml/kg at the end of the treatment phase. The exsanguinating animals had higher blood loss of 5.82, 11.89, and 17.15 ml/kg, blood loss increasing 2-13 times 5 minutes after infusion. Further analysis is being continued to detect any noticeable difference in the exsanguinating animals based on their CBC, ABG, and Luminex assay data.

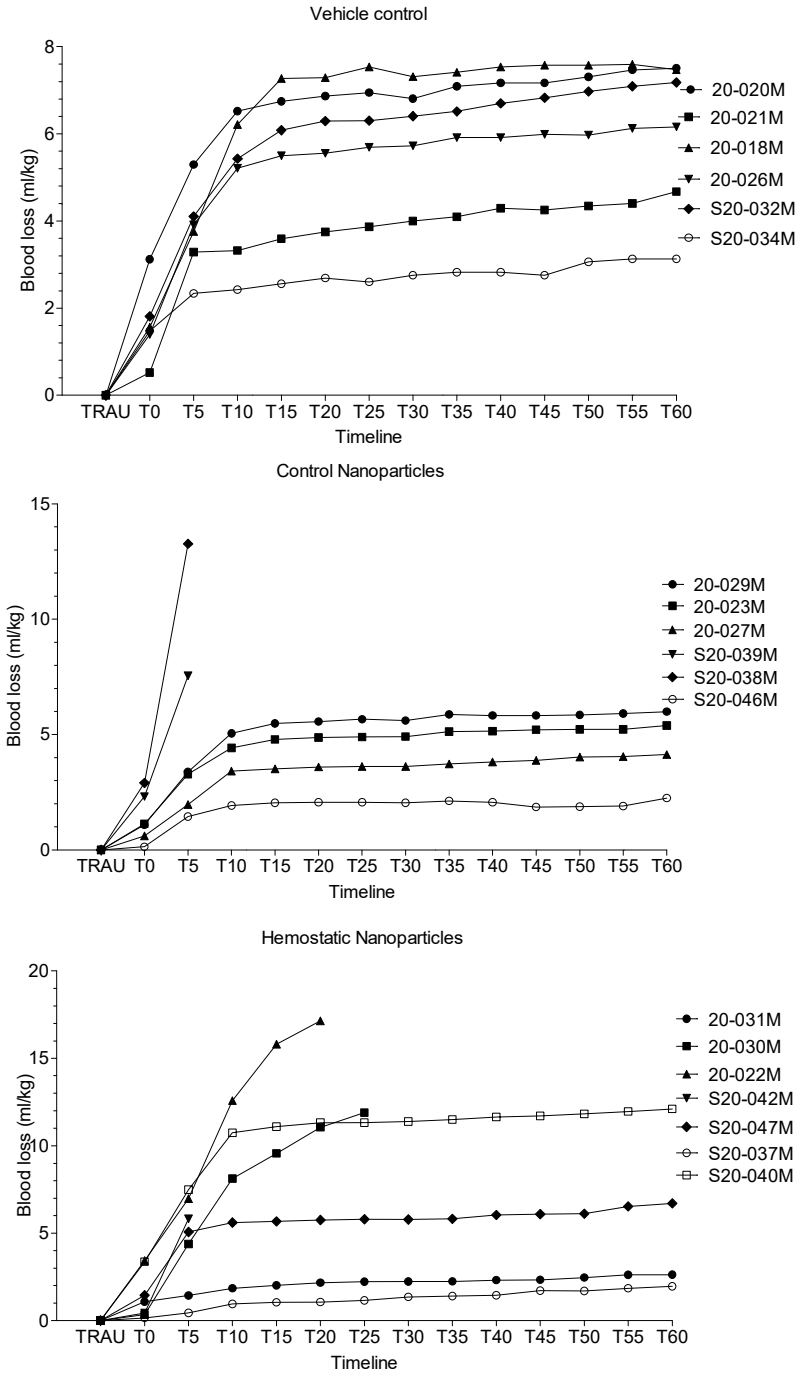

Figure 16: Blood loss per body mass for the injured groups

Applying data-mining principles to discover similarity in trends within groups

To further understand the trend in blood loss and the heterogeneity in the responses observed the groups, further analysis is being carried out in collaboration with data mining scientists. Blood loss captured for three groups of animals was analyzed for this study. Blood loss was tracked right after making an incision from the interval H0 to H4 and T0 to T60. As this data is temporal, we are identifying distributions of time-period where the animals exhibit similar behavior. Similar behavior can be seen in terms of different animals across the three groups showing similar trend in blood loss. Furthermore, temporal analysis is beneficial to see both similarities and deviations in a specific variable in a specific context over the progression of time.

In order to find the similar behavior among the animals we utilized Piecewise Aggregate Approximation(PAA)[29] and SMerg[30] algorithms. PAA provides a summary visualization of the distribution of the data and provide a

snapshot of the overall distribution of the data, looking at the central tendencies over time. In addition to PAA, we used temporal neighborhood discovery technique to identify animals with similar distributions in blood loss. SMerg (Similarity based Merging) is an algorithm used to discover the temporal neighborhood in the data. This algorithm discretizes the data into temporal bins based on similarities which are iteratively identified using a Markov model.

To identify any similarities across animals, we also use K-Means clustering algorithm.[31] It is a popular unsupervised learning algorithm. Here a cluster refers to a collection of data points aggregated together because of similarities across animals or across nanoparticles. Employing clustering on the porcine data provides an insight into which animals demonstrate similar behavior in terms of their blood loss. Alternatively, we can also study which nano particles result in similar outcomes.

Lastly, to study any predictive findings we are exploring the use of class Association rule mining[32] for the in-vivo data to identify if certain nanoparticles or certain blood loss events are predictors of specific outcomes. Our findings from the supervised and unsupervised assessment will result in studying any anomalies that stand out in the patterns discovered and similar behaviors that stand out in the outcomes. We use standard algorithmic metrics such as sum of squared errors, cluster quality (for K-means), confidence, support, and lift (for Class Association rules). We also cross validate findings from the lab to the patterns discovered in the temporal mining. In the future, we also plan to study overlaps across time series distributions by looking at associations across animal studies, to quantify correlations across specific time intervals and also explore delayed correlations.[33-35] We plan to explore the multiple models in an ensemble framework to provide a collaborative outcome from the multiple models.[36]

Discussion

For the first task, we generated hemostatic and control nanoparticles with a higher amount of surface PEG that did not cause an increase in complement protein C5a in vitro in human whole blood and serum. In the second task, infusion of the control and hemostatic nanoparticles did not lead to cardiac anaphylaxis or immediate allergic reactions based on the vitals.

A key feature of complement-mediated hypersensitivity reactions is abrupt changes in the vitals and cardiopulmonary distress. Based on the normalized change in heart rate for each animal, the heart rate from time T=0, i.e., the point of infusion, once stabilized, did not show signs of any additional cardiopulmonary distress, other than the changes that were already present upon the onset of trauma. Hence, the infusion of control and hemostatic nanoparticles did not cause cardiac anaphylaxis, a symptom of complement-mediated hypersensitivity reaction. Abrupt changes in end-tidal CO2 are indicative of the severity of the obstructive respiratory disease, heart failure, pulmonary embolism, and shock.[37] Based on the observations in the inured and uninjured cohorts, there was no abrupt change in end-tidal CO2 compared to end-tidal CO2 observed at baseline other than the sudden drop upon infusion that stabilizes within minutes. The peripheral oxygen saturation is also essential in monitoring cases of hypoxia, and levels below 94% lead to critical condition.[38] The oxygen saturation observations for the injured cohort and uninjured cohort remained close to 100% in the animals receiving the control and hemostatic nanoparticles. Overall, the stable vitals indicate that the nanoparticles did not cause a hypersensitivity reaction upon infusion. However, a glucose spike was observed in some animals receiving the hemostatic nanoparticles. While the ROTEM result for the injured hemostatic nanoparticle group shows a decrease in CT+CFT, the average blood loss per body mass for the group is overall higher for the hemostatic nanoparticles. Looking into the trend for each animal the heterogeneity in the response is also visible.

We are in the process of thoroughly analyzing the data collected during the animal study. Due to heterogeneity in the responses observed, along with the average of response observed for each cohort, we are also analyzing the changes observed in each animal. To better understand the data and determine whether similarities in responses and trends exist within groups we are working in collaboration with data-mining scientists who are applying several tools to understand the central tendencies over time, and also working on understanding the patterns from the overlaps of the time series of individual animals and their different parameters recorded. To further understand the observations, in this quarter, the serum samples collected at various time points are being analyzed to detect changes in complement levels and to investigate whether any changes are observed in parameters that could indicate any signs of hypersensitivity response. The assays

used are for mainly quantifying the histamine levels, the C3 and C3a levels, and investigate if changes in platelet-activating factors (PAF) are visible (by tracking either PAF or the enzyme PAF-AH that controls the activity of PAF).

Reportable Outcomes

As a screening tool for complement activation due to the nanoparticles, we have developed sensitive assays for screening changes in human blood matrices in vitro. This assay is not only applicable for the hemostatic nanoparticles but able to screen such other nanomaterials as well. Moreover, we have focused on understanding the role of surface architecture in complement-mediated hypersensitivity reactions as well. How the PEGylation amounts and PEG linker lengths impact the complement response has been investigated as well.

We have published a manuscript regarding the assay developed for screening nanoparticles in vitro using human blood.[39] We are currently working on writing up our observations regarding role of surface PEG architecture and density, and impact of the PEG linker lengths on the hypersensitivity response in vitro.

Conclusion

Our objective was to determine the optimum surface properties for the hemostatic nanoparticles such that they do not cause any complement-mediated hypersensitivity reaction while augmenting hemostasis. Over the last year, we generated hemostatic and control nanoparticles with a higher amount of surface PEG that did not give rise to C5a in vitro in human whole blood and serum. We then deployed those nanoparticles for intravenous (IV) administration in a large animal (swine) pressure-targeted hemorrhagic shock polytrauma model. From the initial assessment, the hemostatic nanoparticles did not lead to cardiac anaphylaxis or immediate allergic reactions. We are carrying out further analysis of the data collected. We are also working in collaboration with data mining scientists to identify the central tendencies over time and working on understanding the patterns from the overlaps of the time series of individual animals and their different parameters recorded. The interpretations from this study will be critical in developing a clinically translatable formulation of the hemostatic nanoparticles by validating its safety and efficacy.

References

1. Krug, E. G.; Sharma, G. K.; Lozano, R., The global burden of injuries. *American journal of public health* **2000,** *90* (4), 523.

2. Champion, H. R.; Bellamy, R. F.; Roberts, C. P.; Leppaniemi, A., A profile of combat injury. *Journal of Trauma and Acute Care Surgery* **2003,** *54* (5), S13-S19.

3. Cloonan, C. C., Treating traumatic bleeding in a combat setting. *Mil Med* **2004,** *169* (12 Suppl), s8-s10.

4. Heckbert, S. R.; Vedder, N. B.; Hoffman, W.; Winn, R. K.; Hudson, L. D.; Jurkovich, G. J.; Copass, M. K.; Harlan, J. M.; Rice, C. L.; Maier, R. V., Outcome after hemorrhagic shock in trauma patients. *Journal of Trauma and Acute Care Surgery* **1998,** *45* (3), 545-549.

5. Bertram, J. P.; Williams, C. A.; Robinson, R.; Segal, S. S.; Flynn, N. T.; Lavik, E. B., Intravenous hemostat: nanotechnology to halt bleeding. *Sci Transl Med* **2009,** *1* (11), 11ra22 DOI: 10.1126/scitranslmed.3000397.

6. Shoffstall, A. J.; Atkins, K. T.; Groynom, R. E.; Varley, M. E.; Everhart, L. M.; Lashof-Sullivan, M. M.; Martyn-Dow, B.; Butler, R. S.; Ustin, J. S.; Lavik, E. B., Intravenous Hemostatic Nanoparticles Increase Survival Following Blunt Trauma Injury. *Biomacromolecules* **2012,** *13* (11), 3850-3857 DOI: 10.1021/bm3013023.

7. Lashof-Sullivan, M.; Holland, M.; Groynom, R.; Campbell, D.; Shoffstall, A.; Lavik, E., Hemostatic Nanoparticles Improve Survival Following Blunt Trauma Even after 1 Week Incubation at 50 (°)C. *ACS biomaterials science & engineering* **2016,** *2* (3), 385-392 DOI: 10.1021/acsbiomaterials.5b00493.

8. Hubbard, W. B.; Lashof-Sullivan, M. M.; Lavik, E. B.; VandeVord, P. J., Steroid-Loaded Hemostatic Nanoparticles Combat Lung Injury after Blast Trauma. *ACS Macro Letters* **2015,** *4* (4), 387-391 DOI: 10.1021/acsmacrolett.5b00061.

9. Onwukwe, C.; Maisha, N.; Holland, M.; Varley, M.; Groynom, R.; Hickman, D.; Uppal, N.; Shoffstall, A.; Ustin, J.; Lavik, E., Engineering Intravenously Administered Nanoparticles to Reduce Infusion Reaction and Stop Bleeding in a Large Animal Model of Trauma. *Bioconjugate chemistry* **2018,** *29* (7), 2436-2447 DOI: 10.1021/acs.bioconjchem.8b00335.

10. Wibroe, P. P.; Anselmo, A. C.; Nilsson, P. H.; Sarode, A.; Gupta, V.; Urbanics, R.; Szebeni, J.; Hunter, A. C.; Mitragotri, S.; Mollnes, T. E.; Moghimi, S. M., Bypassing adverse injection reactions to nanoparticles through shape modification and attachment to erythrocytes. *Nat Nanotechnol* **2017,** *12* (6), 589-594 DOI: 10.1038/nnano.2017.47.

11. Szebeni, J.; Bedőcs, P.; Csukás, D.; Rosivall, L.; Bünger, R.; Urbanics, R., A porcine model of complement-mediated infusion reactions to drug carrier nanosystems and other medicines. *Advanced Drug Delivery Reviews* **2012,** *64* (15), 1706-1716 DOI: 10.1016/j.addr.2012.07.005.

12. Szebeni, J.; Bedőcs, P.; Rozsnyay, Z.; Weiszhár, Z.; Urbanics, R.; Rosivall, L.; Cohen, R.; Garbuzenko, O.; Báthori, G.; Tóth, M., Liposome-induced complement activation and related cardiopulmonary distress in pigs: factors promoting reactogenicity of Doxil and AmBisome. *Nanomedicine: Nanotechnology, Biology and Medicine* **2012,** *8* (2), 176-184 DOI: 10.1016/j.nano.2011.06.003.

13. Chanan-Khan, A.; Szebeni, J.; Savay, S.; Liebes, L.; Rafique, N. M.; Alving, C. R.; Muggia, F. M., Complement activation following first exposure to pegylated liposomal doxorubicin (Doxil): possible role in hypersensitivity reactions. *Ann Oncol* **2003,** *14* (9), 1430-7 DOI: 10.1093/annonc/mdg374.

14. Wang, G.; Chen, F.; Banda, N. K.; Holers, V. M.; Wu, L.; Moghimi, S. M.; Simberg, D., Activation of Human Complement System by Dextran-Coated Iron Oxide Nanoparticles Is Not Affected by Dextran/Fe Ratio, Hydroxyl Modifications, and Crosslinking. *Front Immunol* **2016,** *7*, 418 DOI: 10.3389/fimmu.2016.00418.

15. Banda, N. K.; Mehta, G.; Chao, Y.; Wang, G.; Inturi, S.; Fossati-Jimack, L.; Botto, M.; Wu, L.; Moghimi, S. M.; Simberg, D., Mechanisms of complement activation by dextran-coated superparamagnetic iron oxide (SPIO) nanoworms in mouse versus human serum. *Particle and fibre toxicology* **2014,** *11* (1), 64 DOI: 10.1186/s12989-014-0064-2.

16. De Sousa Delgado, A.; Léonard, M.; Dellacherie, E., Surface Properties of Polystyrene Nanoparticles Coated with Dextrans and Dextran−PEO Copolymers. Effect of Polymer Architecture on Protein Adsorption. *Langmuir* **2001,** *17* (14), 4386-4391 DOI: 10.1021/la001701c.

17. Fornaguera, C.; Caldero, G.; Mitjans, M.; Vinardell, M. P.; Solans, C.; Vauthier, C., Interactions of PLGA nanoparticles with blood components: protein adsorption, coagulation, activation of the complement system and hemolysis studies. *Nanoscale* **2015,** *7* (14), 6045-58 DOI: 10.1039/c5nr00733j.

18. Ricklin, D.; Lambris, J. D., Complement in immune and inflammatory disorders: pathophysiological mechanisms. *J Immunol* **2013,** *190* (8), 3831-8 DOI: 10.4049/jimmunol.1203487.

19. Benjamini, E., *Immunology: a short course*. Vol. 77.

20. Moghimi, S. M.; Simberg, D., Complement activation turnover on surfaces of nanoparticles. *Nano Today* **2017,** *15*, 8-10 DOI: 10.1016/j.nantod.2017.03.001.

21. Onwukwe, C.; Maisha, N.; Holland, M.; Varley, M.; Groynom, R.; Hickman, D.; Uppal, N.; Shoffstall, A.; Ustin, J.; Lavik, E., Engineering Intravenously Administered Nanoparticles to Reduce Infusion Reaction and Stop Bleeding in a Large Animal Model of Trauma. *Bioconjug Chem* **2018,** *29* (7), 2436-2447 DOI: 10.1021/acs.bioconjchem.8b00335.

22. Hamad, I.; Al-Hanbali, O.; Hunter, A. C.; Rutt, K. J.; Andresen, T. L.; Moghimi, S. M., Distinct polymer architecture mediates switching of complement activation pathways at the nanosphere− serum interface: implications for stealth nanoparticle engineering. *ACS nano* **2010,** *4* (11), 6629-6638.

23. Coty, J. B.; Eleamen Oliveira, E.; Vauthier, C., Tuning complement activation and pathway through controlled molecular architecture of dextran chains in nanoparticle corona. *Int J Pharm* **2017,** *532* (2), 769-778 DOI: 10.1016/j.ijpharm.2017.04.048.

24. Connor, E. F.; Nyce, G. W.; Myers, M.; Möck, A.; Hedrick, J. L., First Example of N-Heterocyclic Carbenes as Catalysts for Living Polymerization: Organocatalytic Ring-Opening Polymerization of Cyclic Esters. *Journal of the American Chemical Society* **2002,** *124* (6), 914-915 DOI: 10.1021/ja0173324.

25. Merle, N. S.; Church, S. E.; Fremeaux-Bacchi, V.; Roumenina, L. T., Complement System Part I - Molecular Mechanisms of Activation and Regulation. *Front Immunol* **2015,** *6*, 262 DOI: 10.3389/fimmu.2015.00262.

26. Merle, N. S.; Noe, R.; Halbwachs-Mecarelli, L.; Fremeaux-Bacchi, V.; Roumenina, L. T., Complement System Part II: Role in Immunity. *Front Immunol* **2015,** *6*, 257 DOI: 10.3389/fimmu.2015.00257.

27. Noris, M.; Remuzzi, G., Overview of complement activation and regulation. *Semin Nephrol* **2013,** *33* (6), 479-92 DOI: 10.1016/j.semnephrol.2013.08.001.

28. Morrison-McKell, T.; Macik, B. G., Point-of-Care Hemostasis Testing. In *Consultative Hemostasis and Thrombosis*, Elsevier: 2013; pp 717-729.

29. Guo, C.; Li, H.; Pan, D. In *An improved piecewise aggregate approximation based on statistical features for time series mining*, International conference on knowledge science, engineering and management, Springer: 2010; pp 234-244.

30. Dey, S.; Janeja, V. P.; Gangopadhyay, A. In *Temporal neighborhood discovery using markov models*, 2009 Ninth IEEE International Conference on Data Mining, IEEE: 2009; pp 110-119.

31. Teknomo, K., K-means clustering tutorial. *Medicine* **2006,** *100* (4), 3.

32. Agrawal, R.; Srikant, R. In *Fast algorithms for mining association rules*, Proc. 20th int. conf. very large data bases, VLDB, 1994; pp 487-499.

33. Liang, Z.; Xinming, T.; Lin, L.; Wenliang, J. In *Temporal Association Rule Mining based on T-Apriori Algorithm and its typical application*, Proceedings of international symposium on spatio-temporal modeling, spatial reasoning, analysis, data mining and data fusion, 2005.

34. Harms, S. K., Temporal Association Rule Mining in Event Sequences. In *Encyclopedia of Data Warehousing and Mining*, IGI Global: 2005; pp 1098-1102.

35. Liang, M.; Xi-Hai, L.; Wan-Gang, Z.; Dai-Zhi, L. In *The generalized cross-correlation Method for time delay estimation of infrasound signal*, 2015 Fifth International Conference on Instrumentation and Measurement, Computer, Communication and Control (IMCCC), IEEE: 2015; pp 1320-1323.

36. Gholap, J.; Janeja, V. P.; Yesha, Y.; Chintalapati, R.; Marwaha, H.; Modi, K. In *Collaborative data mining for clinical trial analytics*, 2015 IEEE International Conference on Bioinformatics and Biomedicine (BIBM), IEEE: 2015; pp 1063-1069.

37. Aminiahidashti, H.; Shafiee, S.; Kiasari, A. Z.; Sazgar, M., Applications of End-Tidal Carbon Dioxide (ETCO2) Monitoring in Emergency Department; a Narrative Review. *Emergency* **2018,** *6* (1).

38. Myatt, R., Pulse oximetry: what the nurse needs to know. *Nursing Standard* **2017,** *31* (31).

39. Maisha, N.; Coombs, T.; Lavik, E., Development of a Sensitive Assay to Screen Nanoparticles in Vitro for Complement Activation. *ACS Biomaterials Science & Engineering* **2020,** *6* (9), 4903-4915 DOI: 10.1021/acsbiomaterials.0c00722.

APPENDICES

A published journal article